2015-10

Integration of Active and Passive Safety Technologies - A Method to Study and Estimate Field Capability

Jingwen Hu, Carol A. Flannagan, Shan Bao
University of Michigan Transportation Research Institute

Robert W. McCoy, Kevin M. Siasoco, and Saeed Barbat
Ford Motor Company

ABSTRACT – The objective of this study is to develop a method that uses a combination of field data analysis, naturalistic driving data analysis, and computational simulations to explore the potential injury reduction capabilities of integrating passive and active safety systems in frontal impact conditions. For the purposes of this study, the active safety system is actually a driver assist (DA) feature that has the potential to reduce delta-V prior to a crash, in frontal or other crash scenarios. A field data analysis was first conducted to estimate the delta-V distribution change based on an assumption of 20% crash avoidance resulting from a pre-crash braking DA feature. Analysis of changes in driver head location during 470 hard braking events in a naturalistic driving study found that drivers' head positions were mostly in the center position before the braking onset, while the percentage of time drivers leaning forward or backward increased significantly after the braking onset. Parametric studies with a total of 4800 MADYMO simulations showed that both delta-V and occupant pre-crash posture had pronounced effects on occupant injury risks and on the optimal restraint designs. By combining the results for the delta-V and head position distribution changes, a weighted average of injury risk reduction of 17% and 48% was predicted by the 50th percentile Anthropomorphic Test Device (ATD) model and human body model, respectively, with the assumption that the restraint system can adapt to the specific delta-V and pre-crash posture. This study demonstrated the potential for further reducing occupant injury risk in frontal crashes by the integration of a passive safety system with a DA feature. Future analyses considering more vehicle models, various crash conditions, and variations of occupant characteristics, such as age, gender, weight, and height, are necessary to further investigate the potential capability of integrating passive and DA or active safety systems.

KEYWORDS – Integrated active and passive safety, Field data, Naturalistic driving data, Computational modeling, Delta-V, Driving posture

---

INTRODUCTION

In general, there are two types of safety systems available in current vehicle designs: passive and active. In addition to active safety systems, driver assist (DA) technologies are becoming more mainstream in the modern vehicle fleet. DA or active safety systems are designed to help drivers avoid or mitigate crashes, whereas, passive safety systems are designed to reduce occupant injury risks during crashes. Until recently, little research regarding integration of these types of systems has been published. Several researchers have estimated fatality and serious injury reduction potential of passive safety systems (e.g., safety belts and airbags) and DA or active safety systems, e.g., forward collision warning and autonomous pre-crash braking (Bean et al. 2009; Evans 1986, 1991; Kahane 1996, 2000; Kusano and Gabler 2010, 2012; NHTSA 1999, 2001). However, such estimations only focused on one of the two systems, separately. With the increasing pace of implementation of DA and active safety systems, features such as pre-crash brake assist or pre-crash autonomous braking provide the potential to affected pre-crash conditions, such as vehicle kinematics (e.g., delta-V) and occupant pre-crash position/posture, both

of which have pronounced effects on occupant injury risks during frontal crashes. Therefore, the potential advantage of an integrated active and passive safety system is not likely to be the sum of these two single systems.

Among the more recent studies, crash safety research has demonstrated that reducing the delta-V can reduce injury risks in frontal crashes. Such strong dependence between crash severity and injury risk has been found through analyses of real-world crash data (Augenstein et al. 2003; Kononen et al. 2011) and data from event data recorders (Stigson et al. 2012). Current passive safety systems have to be designed with consideration of regulatory and/or third party crash testing conditions, in which the delta-Vs are 35 mph or higher in frontal crashes. While some studies have shown that achieving top ratings in these types of tests generally results in lower risks of death in real-world crashes (Farmer 2005; Ryb et al. 2010), other studies have also reported that no statistically significant relationship between the Euro NCAP scores and real-world death or severe injury outcomes (Segui-Gomez et al. 2007, 2010). Therefore, a passive safety system that can adapt to a lower delta-V resulting from the activation of a particular active safety device may further reduce occupant injury risks. The reduced delta-V resulting from a DA or active safety system is generally from a hard pre-crash braking event. The braking events can potentially affect the occupant pre-crash postures, most importantly the head locations right before the crash. A previous modeling study by Bose et al. (2010) has demonstrated that occupant pre-crash posture has significant effects on occupant injury risks in frontal crashes, and more recent studies (Adam and Untaroiu 2011; Untaroiu and Adam 2012) have also shown that passive safety systems that can adapt to occupant pre-crash posture may further reduce occupant injury risk. Therefore, if the occupant pre-crash posture is changed significantly due to the DA or active safety system, then occupant injury risk may potentially be further reduced by an integrated active and passive safety system that is adaptable to such occupant posture changes.

In order to adapt the passive safety system to the changed pre-crash conditions caused by the DA or active safety system, signals from active safety system, such as the delta-V and pre-crash posture information, should be integrated into the passive safety system, so that their performance can be tailored to the changed crash and occupant situations. Majority of the recent studies on integration of active and passive safety technologies focused only on reversible seatbelt pretensioner (Ito et al. 2013; Komeno et al.

2013; Mages et al. 2011; Merz et al. 2013), which can pull the seatbelt webbing into the retractor during a pre-crash braking. Studies on quantifying the benefit of developing a restraint system truly adaptive to the delta-V and occupant posture resulted from activation of a pre-braking DA feature are lacking in the literature.

Therefore, the objective of this study is to assess the potential occupant protection capabilities of integrated active and passive safety systems. Specifically, in this study, a combination of field data analysis, naturalistic driving data analysis, and computational simulations were used to explore the potential occupant protection capabilities of a restraint system adaptive to the pre-crash delta-V and occupant posture. The following steps were required in this study:

1) Identifying the patterns of pre-crash vehicle kinematic changes (e.g. delta-V change) when a DA or active safety system is presented through a field data analysis.
2) Identifying the patterns of pre-crash occupant postures when a DA or active safety system is presented (e.g. pre-crash braking) through a naturalistic driving data analysis.
3) Performing computational simulations to evaluate injury risk reduction if the restraint system design is optimized with a given delta-V and pre-crash occupant posture.
4) Estimating the weighted average of injury risk reductions of integrated safety systems considering the delta-V change and pre-crash posture change due to the presence of a DA or active safety system.

FIELD DATA ANALYSIS

In this study, national crash datasets were analyzed to better understand the scope of the passive safety issue addressed by a given active safety system. Potential injury risk reduction for an active safety system comes in two types: crashes avoided and crashes mitigated. For crashes avoided, there is no further work for the passive safety system to do, but there are also fewer crashes to be addressed by the passive safety system. However, for crashes mitigated, the passive safety system may further reduce the occupant injury risks by preparing seat belts and/or airbags for a potential crash. Injury risk reduction estimation must therefore focus on the potential enhancement of passive safety system in the context of the crash mitigation resulted by the active safety system.

In this study, the purposes of the field data analysis were 1) to estimate the delta-V distributions in frontal crashes with and without a DA or active safety system, and 2) to provide a weighting function for computational simulation results, so that the potential injury risk reduction of integrated active and passive safety systems can be estimated for the whole population.

Methods

Data from the National Automotive Sampling System (NASS) were used in the field data analysis. NASS includes two datasets—the General Estimates System (GES) and the Crashworthiness Data System (CDS). The GES database is a complex stratified probability sample of police-reported crashes in the United States. It contains about 50,000 crashes per year, and each is coded in a standardized way. Only information from police reports is included, but the sample allows general estimation of the scope of the crash problem across the country. The CDS database is a complex stratified sample of tow-away crashes involving a light vehicle in the United States (National Highway Traffic Safety Administration, 2007). CDS captures 3000-4000 crashes per year and includes a full crash investigation, including estimation of delta-V, the change in speed experienced by a given vehicle involved in a crash. Delta-V is critical to this effort because it is the single strongest predictor of injury outcome and because crash mitigation by a DA or active safety feature is assumed as a reduction in delta-V.

GES provides information about the overall scope of the rear-end crash scenario, which we found makes up about 34% of all police-reported crashes. The rear-end crash defined here is a crash wherein a vehicle crashes into the vehicle in front of it. To avoid confusion, we will use "frontal crash(s)" to represent this type of crashes throughout the paper. One of the challenges in this work is that while the GES database is the key to understand the broad scope of the crash problem addressed by the active safety system, the detail in CDS is needed to estimate the delta-V distribution and injury outcome from these crashes. To address this, a previously developed method of estimating the delta-V distribution using injury outcome in GES and a known relationship between delta-V and injury based on the CDS data (Flannagan 2013) was used (see Appendix A). This can be thought of as "reverse-engineering" the delta-V distribution for a given crash direction based on the distribution of injuries seen in the GES crash data. Note that this method does not reconstruct delta-V for a single crash, but instead generates a distribution of delta-V over a large number of crashes of a given type.

Results

Figure 1 shows the estimated delta-V distribution for the striking vehicle in a frontal crash. The distribution is lognormal, which has been found to fit known delta-V distributions reasonably well. This distribution has a mean of 2.85 and a standard deviation of 0.50.
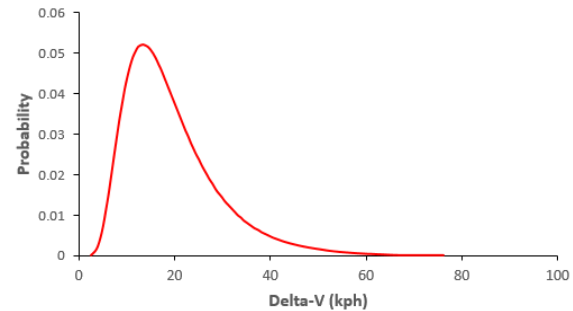

Figure 1: Distribution of delta-V a frontal crash

This distribution (and the overall 34% of all police-reported crashes representing frontal crashes) makes up the base, or denominator, to which active and passive safety systems effectiveness estimates are compared. Since the passive safety system, by definition, operates with the presence of a DA or active safety system, next it is needed to find the estimated effectiveness of an active safety system for crash avoidance. Since it is a difficult and elusive problem to estimate the effectiveness of an active safety system in the scope of this project, several estimates in a sensitivity analysis were used. In this study, a 20% effectiveness for crash avoidance for a DA or active safety system was assumed and used as an example.

The overall percent reduction in crashes does not, in and of itself, determine how the delta-V distribution should change. However, it is safe to assume that if some percentage of crashes is avoided, others are mitigated, or reduced in severity. Thus, the delta-V distribution of frontal crashes for vehicles equipped with a DA or active safety system will not be the same, but with smaller area under the curve.

To address this, two different models—a simple, straw-man model of the reduction process, and a more complex model were investigated. The first model simply applies a fixed delta-V reduction to the entire delta-V distribution with the goal of eliminating 20% of the area under the curve. This approach is illustrated in Figure 2.
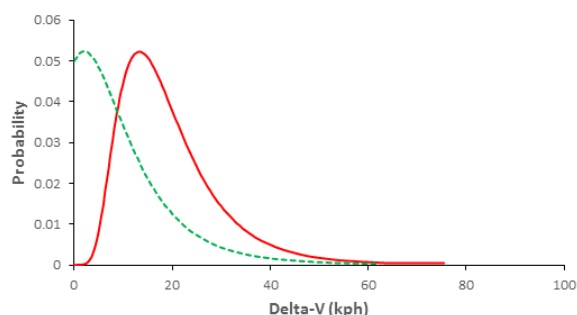
Figure 2: Original distribution of delta-V for the striking vehicle in a frontal crash (solid curve) and hypothetical distribution of delta-V for DA active-safety-equipped vehicles (dash curve), based on a fixed delta-V reduction for all crashes.

The fixed curve shift shown in Figure 2 meets the goal of eliminating 20% of crashes, and it would serve as a good model for the effect of an automated braking system on the delta-V distribution. However, it does not represent a satisfying mechanistic model for the scenario in which the driver is responding to a warning or even for a brake-assist system that works only after the driver has initiated braking. A more plausible model of the effect of a DA or forward collision warning system is that for each frontal crash situation, the driver response to the warning is itself a random variable with an exponential distribution. The exponential distribution is a common distribution of wait times, so it makes sense in this context. We call this the random-shift model. Again, the parameter of the driver response distribution is selected so that 20% of the area under the curve is to the left of 0 delta-V (i.e., the crash is avoided). The computation of the exponential parameter is explained in Appendix B. Figure 3 shows the random-shift delta-V distribution compared to the original distribution.
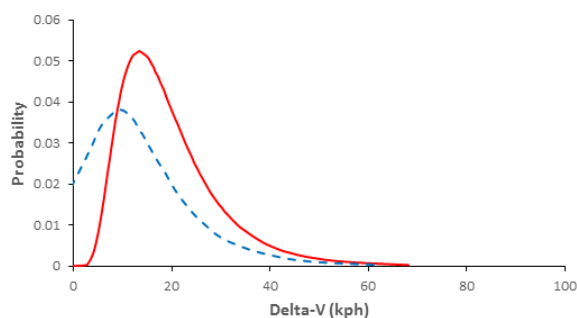

Figure 3: Shifted distribution of delta-V for the striking vehicle in a frontal crash (solid curve) and hypothetical distribution of delta-V for DA active-safety-equipped vehicles (dash curve), based on a random delta-V reduction for all crashes.

A further refinement of the random-shift model is one that incorporates differences in response time as a function of age. Age influences this problem in a variety of ways. First, frontal crashes involve drivers of different age groups at different rates. Second, drivers in different age groups may have different original delta-V distributions for frontal crashes. Finally, different-age drivers may have different response times to warnings. These age-related differences are particularly important because age has a strong effect on injury risk, and passive safety systems might be tuned to the population of drivers and passengers who are likely to be encountered.

Using GES, we estimated the percent of frontal crashes involving drivers in each of three age groups: young (16-30), middle-aged (31-59), and older (60+). Of drivers of the striking vehicle in a frontal crash, 39% are young, 48% are middle-aged, and 13% are older. This largely represents the total driving exposure for these groups, but for the young drivers in particular, there is an increased risk of being in a frontal crash.

Next, using CDS data, we estimated the delta-V distribution differences for each of these age groups. In particular, young drivers tend to have a higher mean delta-V, followed by middle-aged drivers, and then older drivers. The three resulting delta-V distributions are shown in Figure 4. These curves represent the current population of frontal crashes, broken down by driver age group. The area under each curve represents the contribution of those drivers to the total population. Thus, the sum of the areas under all three curves is 1.0.
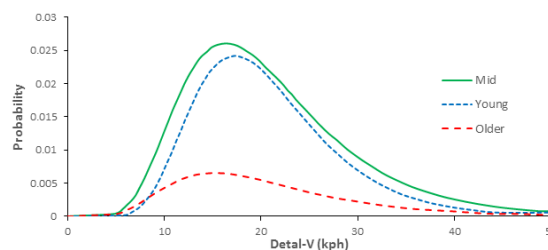

Figure 4: Original distribution of delta-V for the striking vehicle in a frontal crash, broken down by driver age group. Area under each curve represents the percent of crashes involving each driver age group. The total area under all curves is 1.0.

Figure 4 represents both the differential involvement in frontal crashes and different delta-V distributions. However, investigation of the literature on the third difference—warning response time—produced mixed results. Studies by Kramer et al. (2007) and Lerner (1993) both showed no difference as a function of age

in response to warnings. Our own data analysis of warning response also showed no difference in response time. In this study, we recommend continuing the estimation without a reaction-time difference by group.

Using a random shift with equal response distributions for all age groups, we estimated the distribution of delta-V for DA active-safety-mitigated frontal crashes by age group as shown in Figure 5. Note that it is assumed a 20% crash avoidance by a DA or active safety systems.
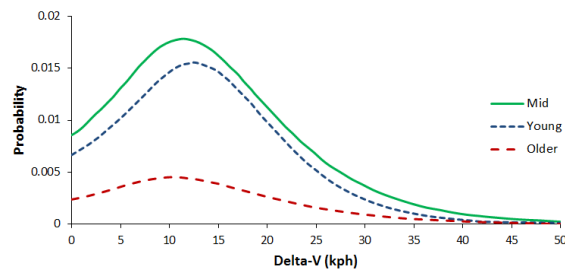

Figure 5: Shifted distribution of delta-V for the striking vehicle in a frontal crash for DA active-safety-equipped vehicles, broken down by driver age group. Area under each curve represents the percent of crashes involving each driver age group. Total area under all curves is 0.8.

NATURALISTIC DRIVING DATA ANALYSIS

The purpose of the naturalistic driving data analysis in this study is to provide data and compare the drivers' head positions before and after the onset of hard braking events using data from the Integrated Vehicle Based Safety System (IVBSS) program recently completed by UMTRI (Sayer et al. 2011). Drivers' head position was used as a reference to their body position during hard braking events (i.e., critical safety events). It is expected that the observed head position change for different driver groups will have different trends.

Dataset

The IVBSS project was a five-year large-scale study that was conducted by UMTRI and funded by US DOT. In that study, a total of 108 randomly sampled, passenger-car drivers participated, with the sample being stratified by age (younger from 20 - 30 years; middle-aged from 40 - 50 years; older from 60 - 70 years) and gender (female and male). Sixteen late-model Honda Accords were used as research vehicles. Consenting drivers used the test vehicles in an unsupervised manner, simply pursuing their normal

trip-taking behavior over a 40-day period, using the equipped vehicles as a substitute for their own personal vehicles. The first 12 days of vehicle use served as the baseline period during which warning functions were not provided to drivers, but all sensors and equipment were still operating in the background and all data was recorded. The following 28 days were the treatment period during which warning functions were enabled and provided to drivers when appropriate. The integrated warning system includes forward-crash, lateral-drift, lane-change/merge crash, and curve-speed warnings. The data set collected represents 213,309 miles, 22,657 trips, and 6,164 hours of driving, with over 600 signals captured at 10 Hz or faster (e.g., speed, range, throttle position, and radar data). There are five camera views to capture drivers' head, forward scene, hand position, left and right rear views (Figure 6).
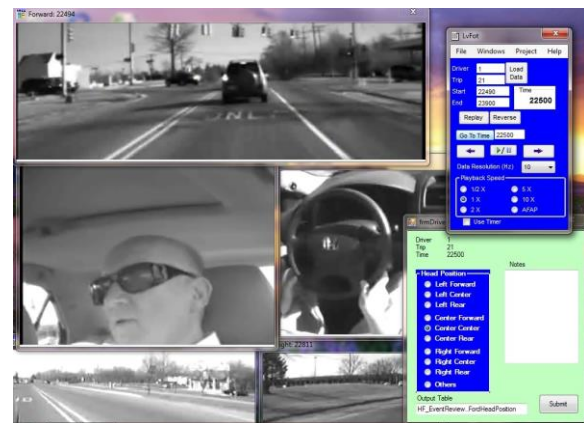

Figure 6: Five camera views from IVBSS study

Methods

The definition of hard braking events was determined based on both the G-force level that was commonly used in the literature, and the G-force distribution in our datasets, which was defined as a braking profile with a peak deceleration level of 0.45g or more. The video data from these events were analyzed to quantify the patterns of pre-crash occupant postures, especially head locations. Within the IVBSS datasets, a total of 470 hard braking events were identified.

Table 1 shows the distribution of the hard braking events across different age and gender groups. The young male drivers had the highest proportion of hard braking events. The density distribution of the deceleration G-levels of all the 470 hard braking events was shown in Figure 7. In about 85% of the hard braking events, the maximum deceleration value was between 4.5 and 5.5 m/s^2.

Table 1: Number of hard braking events by age and gender

	Younger	Middle-aged	Older	Total
Female	61	53	63	177
Male	158	73	62	293
Total	219	126	125	470
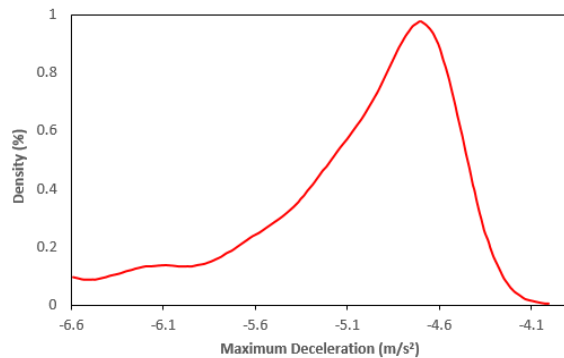
Figure 7: Distribution of peak deceleration (m/s^2)

Drivers' head position (5s before and 5s after the brake onset) were video coded and classified into 10 categories: left forward, left center, left rear, center forward, center center, center rear, right forward, right center, right rear, and others (Figure 6). The coding software was designed and developed for the purpose of this study. Two trained video coders were working in parallel on all the 470 hard braking events. Their results were cross compared and both coders revisited all the events on which they had different opinions till they both agreed on the final results.

Due to the small sample size, data on drivers' head position was further aggregated into four levels including Forward (i.e., drivers' body leaning forward), Centered (i.e., drivers' body remaining straight), Rearward (i.e., drivers' body leaning rearward), and others (e.g., looking down to cell phones) for the analysis. Example of different head positions was shown in Figure 8.

The dependent variable was the percentage of time that each driver spent in each position level during each braking event. The analyses were performed with linear mixed models using the PROC MIXED procedure in the statistical software package SAS 9.2 (Eq 2). An unstructured covariance matrix was assumed to model variance heterogeneity and to account for within-subject variance from repeated observations from the same driver. Fixed effects predictors included age, gender, head position level, and timing (before or after brake onset). Driver and interactions between driver and any fixed effects were

treated as random effects. This accounts for within-subject variance from repeated observations from the same driver and effectively compares a driver to him/herself.

$$Y = \alpha + \beta X + \mu Z + \varepsilon \quad (2)$$

Where,

- Y=Percentage of time that each driver spent in each head position level,
- α=intercept,
- β=coefficient matrix for the fixed effects,
- X=fixed effects (e.g., age, gender),
- μ=coefficient matrix used for random effects matrix,
- Z=random effects matrix (e.g., subject effect), and
- ε=error term (normally and independently distributed) associated with parameters not included in the model.
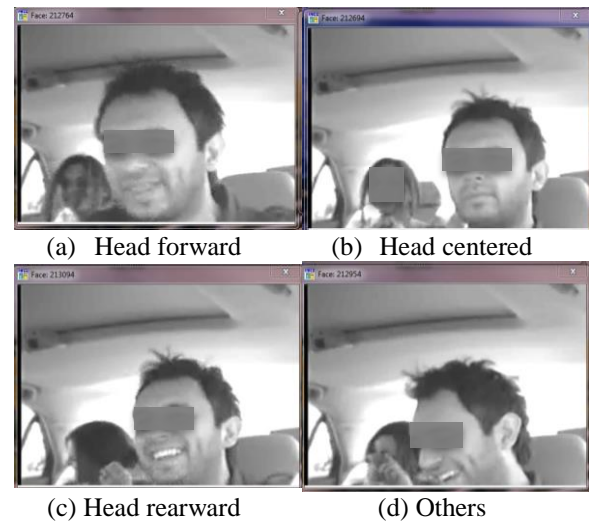

(a) Head forward   (b) Head centered

(c) Head rearward   (d) Others

Figure 8: Examples of different driver head locations

Results

Results of the analysis showed a significant interaction term between position and timing (F(3,402)=11.7, p<0.05). As shown in Figure 9, drivers' head position were mostly in the center position before the braking onset, while the percentage of time drivers leaning forward or backward were increased significantly after the braking onset. Age effect was observed that the percentage of time spent in the other position of young drivers was significantly higher than the other two age groups, suggesting young drivers were more likely engaging in non-driving tasks. The percentage of time that older drivers spent in centered position was significantly higher than the other two driver groups (Figure 10).
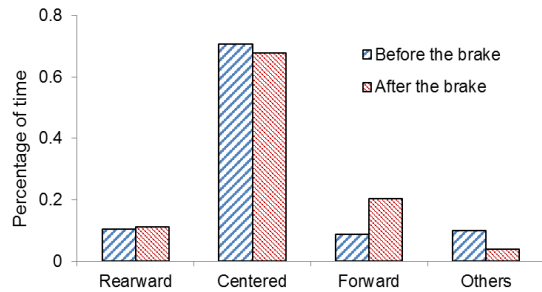
Figure 9: Timing effect on the percentage of time spent in each head position
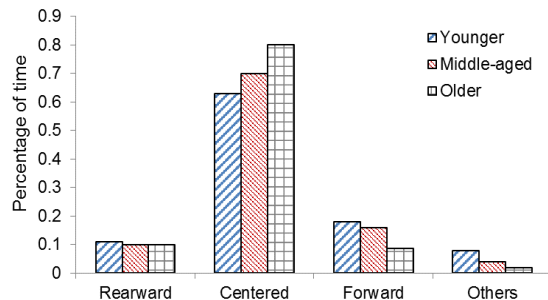

Figure 10: Age effect on the percentage of time spent in each head position

Analysis on drivers' head position changing patterns from before-braking-onset to during-braking was also conducted. Data during the last second before the braking onset and the first second after the brake onset of the 470 hard braking events were extracted and used in the analysis. Three main changing patterns were observed, from centered to forward position, from centered to rearward position and stay centered. All drivers tend to be more likely leaning forward during the first second of braking. A significant age effect was observed ($F_{(2, 405)} = 8.7$, $p < 0.05$) that both young and middle-aged drivers tend to more likely to lean forward after they stepped on the brake pedal when compared to older drivers (Figure 11).
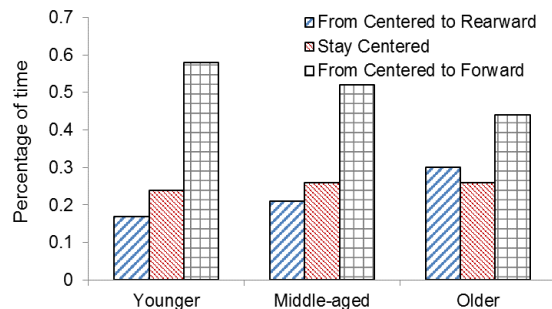

Figure 11: Age effect on the head position changing pattern

COMPUTATIONAL MODELING

In this study computational models were used to estimate the potential reduction of occupant injury risks with the integrated active and passive safety system comparing to those without such a system. In particular, a DA or active safety system may reduce the delta-V of a crash, and at the same time may also affect the pre-crash occupant posture due to the hard braking before the crash. Therefore, in this study, simulations were conducted with different pre-crash occupant postures under different delta-V levels, so that the effects from active safety system can be evaluated. Furthermore, design parametric studies and optimizations were also performed under each combination of occupant posture and delta-V condition. The minimal injury risks with the optimal design system in each crash condition were compared to those with the baseline (current) design. Consequently the injury risk reduction potential of an optimized design system considering the occupant posture and delta-V levels (two factors affected by the active safety system) can be estimated.

Model Development and Validation

As shown in Figure 12, a MADYMO ATD model and a MADYMO human model integrated in a generic vehicle and restraint system model were used as the baseline models to quantify the occupant injury outcomes. The ATD model is the HIII 50th percentile male model, while the MADYMO human model is a rigid-body based human facet model representing a 50th percentile male occupant. The vehicle occupant compartment model, including the driver airbag, knee airbag, seat, steering wheel, instrument panel, and other interior components, was provided by Ford Motor Company, while the seat belt system model, including the webbing, retractor, pretensioner, and load limiter, is based on a production seat belt system provided by TRW.

The HIII 50th ATD model has been rigorously validated against ATD calibration tests and sled tests, while the human model has been validated extensively at component level and full body level against volunteer (low to mid impact severity) and PMHS test data (mid to high impact severity) (TASS 2012).

The ATD model, occupant compartment model and restraint system models were further validated against US-NCAP test data provided by Ford. The comparison of the ATD and seat belt responses (horizontal and vertical head, chest, and pelvis accelerations, shoulder and lap belt forces, and chest deflection) between the test and simulation are shown in Figure 13. Good correlation has been achieved.
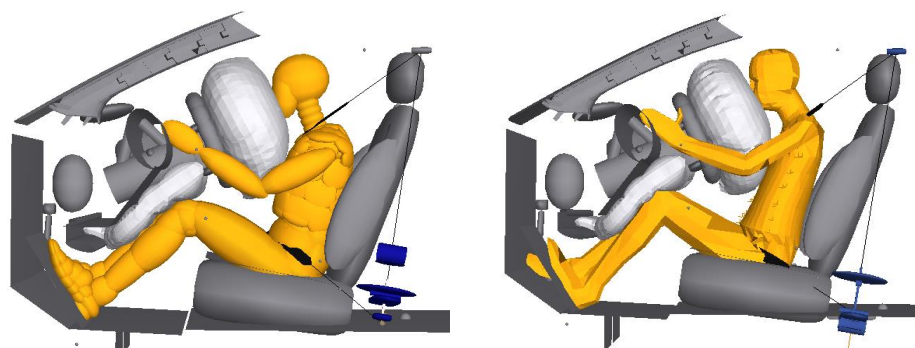
(a) Driver compartment and ATD model   (b) Driver compartment and human model
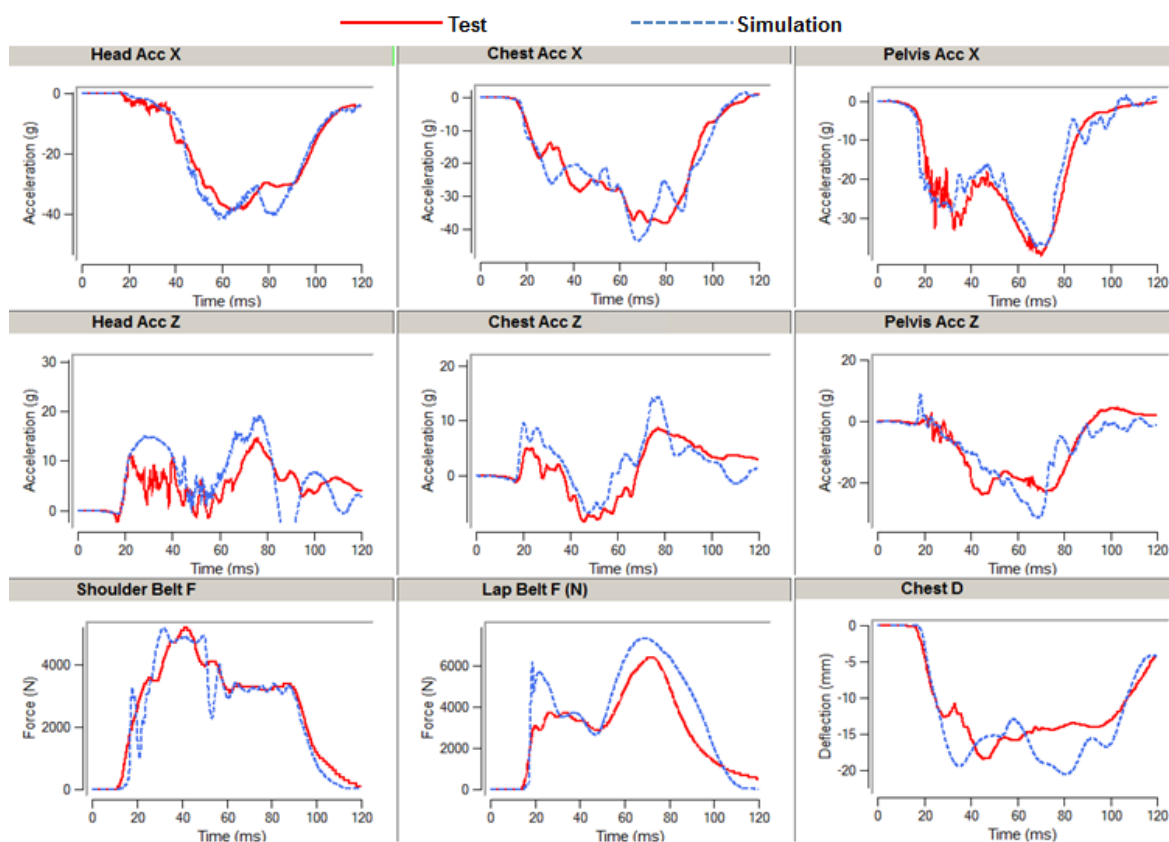Figure 12: MADYMO ATD, human, driver compartment, and restraint system models

Figure 13: Model validation against US-NCAP test data

Injury measures and risk curves between ATD and human models

Because no cadaver tests are available with the Ford vehicle model, the human model responses in the specific vehicle model cannot be validated. To ensure the validity of the interaction between the human model and the vehicle model, injury outputs from the ATD model and the human model were compared.

In this study, injury risks for the head, neck, chest, and femur were calculated based on the injury risk curves shown in Table 2. A single joint probability of injury (Eq 3) combining all four injury risks was also calculated as the main output, which is originally used for assigning the star rating in the US-NCAP tests.

$$P_{joint}=1- (1-P_{head}) \times (1-P_{neck}) \times (1-P_{chest}) \times (1-P_{femur}) \quad (3)$$

Table 2: Injury risk curves used in this study

	HIII 50th ATD Model	**50th Human Model**
Head (HIC15)	$P_{head}(AIS3+) = \emptyset \left(\dfrac{ln(HIC15) - 7.45231}{0.73998} \right)$ Where Φ=cumulative normal distribution	
Neck (Nij and tension/compression in kN)	$P_{Nij}(AIS3+) = \dfrac{1}{1 + e^{3.2269-1.9688Nij}}$ $P_T(AIS3+) = \dfrac{1}{1 + e^{10.9745-2.375T}}$ $P_C(AIS3+) = \dfrac{1}{1 + e^{10.9745-2.375C}}$ $P_{neck} = Max(P_{Nij}, P_T, P_C)$	
Chest (deflection in mm)	$P_{ch}(AIS3+) = \dfrac{1}{1 + e^{10.5456-1.568*D^{0.4612}}}$	$P_{ch}(AIS3+) =$ $\dfrac{1}{1+e^{10.5456-1.568*(D/1.5)^{0.4612}}}$ *
Femur (force in kN)	$P_{femur}(AIS2+) = \dfrac{1}{1 + e^{5.795-0.5196F}}$	

* A different chest injury risk curve was used for the human model to that used for the ATD model, because the MADYMO human model is over-predicting the chest deflection. The adjusted chest injury risk curve is based on a chest deflection comparison between the MADYMO human model and a finite element human model (THUMS 4.0). Using the adjusted injury risk curve, the human-model-predicted chest injury risks can better match those from the field. More details on adjusting the chest injury risk curves are attached in the Appendix C.

Table 3: Model predicted injury measures for ATD and human models in a 35mph frontal crash with different seating postures

Pre-crash posture	Head Forward (–200 mm)				Head Normal (0mm)				Head Rearward (+60mm)			
	ATD		Human		ATD		Human		ATD		Human	
Figure												
	Val.	Prob.	Val.	Prob.	Val.	Prob.	Val.	Prob.	Val.	Prob.	Val.	Prob.
HIC Phead	206	0.20%	267	0.58%	166	0.08%	245	0.42%	309	1.01%	358	1.68%
Chest D (mm) Pchest*	19.2	1.19%	49.5	6.43%	19.8	1.30%	58.5	11.4%	21.0	1.54%	59.2	11.9%
NIJ Pneck	0.35	7.32%	0.32	6.96%	0.34	7.19%	0.41	8.20%	0.33	7.06%	0.42	8.38%
Femur F (kN) Pfeumur	1.55	0.68%	4.03	2.41%	1.27	0.59%	2.46	1.08%	1.00	0.51%	3.78	2.13%
Pjoint*	9.23%		15.54%		9.00%		19.90%		9.87%		22.33%	

* Different chest injury risk curves were used between the ATD and the human model, and Pneck was removed from the Pjoint in the following parametric study.

Table 3 shows the simulated ATD and human injury outputs and their associated injury risks with three seating postures (head forward 200 mm, normal driving posture, and head rearward 60 mm) under a 35 mph NCAP crash pulse. The head (HIC) and neck (NIJ) injury outcomes are consistent between the ATD and human models, but the chest deflection and femur forces are significantly different. In particular, the human model predicted much higher chest deflection and femur forces than those from the ATD model. A recent study by Digges et al. (2013) compared the injury risks in 302 NCAP tests and the injury risks for NCAP-like crashes in the NASS-CDS database as shown in Table 4. The NCAP tests significantly underestimated the chest and knee-thigh-hip (KTH) injury risks. For this reason, the higher chest deflection and femur forces predicted by the human model may represent the field data better than the ATD model. The MADYMO human model significantly over-estimated the chest injury risks, if the same chest injury risk curve as that used for the ATD was applied. Therefore, the chest injury risk curve was adjusted for the MADYMO human model to better match the field data. Specifically, the chest deflections predicted by the MADYMO human model was scaled down by 1.5 times for injury risk calculation. Details on chest injury risk curve adjustment are attached in the Appendix C.

Furthermore, results in Table 3 and Table 4 also show the following trends:

- Both the ATD and human models showed that a normal driving posture led to the lowest HIC value among three postures, while postures beyond normal would increase the HIC value.
- Both the ATD and human models showed that a posture with a more rearward head location increased the chest deflection.
- The head location did not affect NIJ-associated neck injury risks significantly, and such risks were generally too high compared to the field data. As a result, in the following parametric studies, Pneck was removed from the equation to calculate Pjoint.
- Even though human model predicted higher KTH injury risks than the ATD model, they are still much lower than those in the field.
- The ATD model predicted the lowest total injury risk (Pjoint) in the normal driving posture, while the human model predicted that the more rearward the head, the higher the total injury risk (Pjoint).

Table 4: Comparison of injury risks derived from NASS field data with those derived from NCAP tests (Driver Only)

Body Region	NASS Mid-Bound	NCAP 2011 Risk Functions
Neck-Spine 3+	0.70%	7.90%
Head-Face 3+	3.2%	2.3%
Chest 3+	10.6%	6.8%
Knee-Thigh-Hip (KTH) 2+	14.0%	4.9%
NCAP (Any)	20.9%	20.1%

Note: Table from (Digges et al. 2013)

Design parameters, crash pulses, and safety feature firing time

Table 5 shows the parameters being used in the current study. This list covers the design parameters related to the knee bolster, steering column, driver airbag, and seatbelt. Occupant head position and vehicle delta-V are the two confounding parameters in the parametric study, which are related to the DA or active safety system. The crash pulses used in this study are based on the real vehicle crash test data provided by Ford at different impact velocities as shown in Figure 14. The airbag, steering column, and seatbelt pre-tensioner fire times at different impact velocities were also provided by Ford and are shown in Table 6.
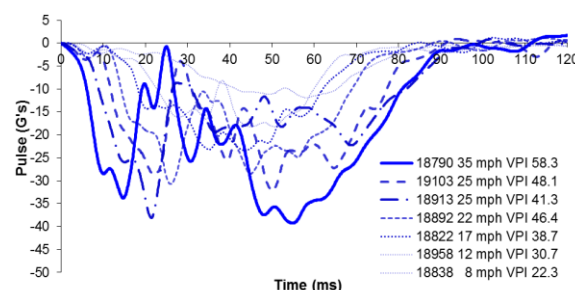
Figure 14: Crash pulses at different delta-Vs

Parametric study setup

To enable large-scale parametric analyses, an automated computer program were developed using a combination of MADYMO, ModeFRONTIER, and other in-house programs to vary the restraint configurations and conduct injury risk evaluations. Similar work has been done previously in optimizing restraint system for occupants with various ages and sizes (Hu et al. 2013a; Hu et al. 2013b). In this study, 3 crash speeds (35mph, 25mph, and 17mph) and 4 occupant postures with different head locations (forward-200mm, forward-100mm, normal, and rearward-60mm) were simulated, which resulted in 12

parametric studies using the ATD model and another 12 parametric studies using the human model. The simulation framework for each parametric study was created in ModeFrontier, in which 10 design parameters were varied within the ranges provided in Table 5 and injury measures on the head, neck, chest, and lower extremities were estimated. The injury measures of head, chest, and lower extremities were used to calculate the Pjoint. In each parametric study, 200 simulations were sampled using the Uniform Latin Hypercube Sampling (ULHS) method for a given occupant pre-crash posture and crash delta-V level. This sampling method provides a uniform distribution of restraint conditions in the design space. In total, 2400 simulations were conducted with the MADYMO ATD model, and 2400 simulations were conducted with the MADYMO human model.

Results of the parametric studies

As an example, the ATD-model-predicted Phead (based on HIC) and Pchest (based on chest deflection)

subjected to the 35mph crash pulse with 4 pre-crash postures are shown in Figure 15, in which the yellow star represents the baseline design, and the red star represents the optimum with the lowest Pjoint among the 200 restraint design configurations. In the "normal driving" and "head rearward" postures, even though the baseline design did not provide the lowest Pjoint, they were very close to the parietal optimal line. In other words, the baseline design could be considered as one of the optimal solutions in reducing the occupant head and chest injury risks in these two pre-crash posture conditions. The results shown in Figure 15 confirmed that the baseline design has been optimized in the "normal driving" posture condition. On the other hand, the baseline design does not provide the optimal occupant protection when the driver is in "head forward" pre-crash postures. Table 7 shows the injury risks from the baseline design and the optimal design predicted by the ATD model for all 12 delta-V*posture conditions.

Table 5: Design parameters in the parametric study

	Variables	**Range**
Occupant	Occupant head position from nominal (mm)	-200 (forward) - +60 (rearward)
Vehicle	Crash Pulse	Figure 14
Knee Bolster	Bolster stiffness scale	35% - 100%
	Bolster placement (m)	nominal, -0.050, -0.075
Steering Column	Column force scale	30% - 100%
	Column stroke (m)	0.010 - 0.100
Airbag	Vent size scale	60% - 140%
	Fire time/delay (ms) *	Table 6
	Tether length (m)	0.2032 - 0.3232
	Smiley tether length (m)	0.08 – 0.16
Seatbelt	Load Limit (kN)	2.0 – 4.0
	Pre-tensioner Firing time (ms) *	Table 6
	Webbing length (mm)**	Corresponding to the head location

* - Airbag and seatbelt pre-tensioner firing time were varied with delta-V, but were not used to optimize the occupant protection. ** - The webbing length was adjusted based on the head/shoulder location for each simulation.

Table 6: Airbag, steering column, and seatbelt pre-tensioner fire time (ms)

Speed (mph)	VPI	APT	RPT	KAB	DAB Stage 1	DAB Stage 2	Adaptive Steering Column
35	58.3	15.0	10.0	10.0	11.5	16.5	11.5
25	48.1			17.5	17.5	22.5	
25	41.3			12.5	15.5	20.5	
22	46.4			19.5	20.5	25.5	
17	38.7	28.5	23.5	23.5	24.5	174.5	24.5
12	30.7			26.0	27.0	177.0	27.0
8	22.3	0.0	0.0	0.0	0.0	0.0	0.0

*VPI: Vehicle Pulse Index, APT: Anchor Pre-tensioner, RPT: Retractor Pre-tensioner, DAB: Driver Airbag
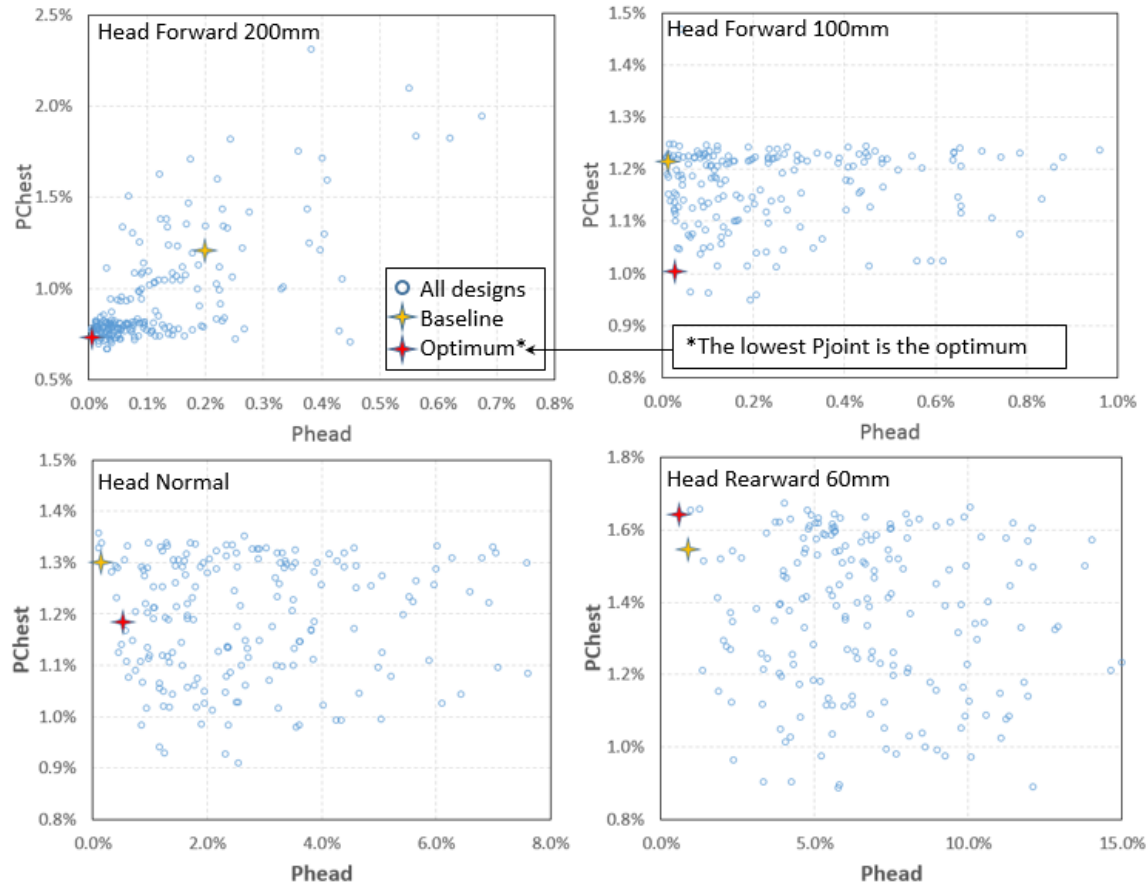
Figure 15: ATD-model-predicted Phead and Pchest for 200 designs under the 35 mph crash pulse

Table 7: ATD model-predicted injury risks for the baseline and optimal designs

		Head Forward (–200mm)		Head Forward (–100mm)		Normal (0 mm)		Head Rearward (+60mm)	
		Baseline	Optimal	Baseline	Optimal	Baseline	Optimal	Baseline	Optimal
35mph	Phead	0.20%	0.01%	0.03%	0.03%	0.08%	0.10%	1.01%	0.64%
	Pchest	1.19%	0.73%	1.24%	1.01%	1.30%	1.33%	1.54%	1.64%
	Pneck	7.32%	6.49%	7.88%	5.76%	7.19%	8.31%	7.06%	6.47%
	Pfemur	0.68%	0.44%	0.65%	0.42%	0.59%	0.43%	0.51%	0.43%
	Pjoint	2.06%	1.17%	1.91%	1.44%	1.95%	1.85%	3.03%	2.69%
25mph	Phead	0.42%	0.07%	0.06%	0.00%	0.06%	0.01%	0.18%	0.07%
	Pchest	0.90%	0.56%	1.07%	0.80%	1.28%	0.88%	1.00%	0.83%
	Pneck	7.32%	7.13%	7.19%	6.21%	7.06%	6.35%	6.68%	5.87%
	Pfemur	0.64%	0.54%	0.52%	0.46%	0.53%	0.45%	0.52%	0.45%
	Pjoint	1.94%	1.17%	1.65%	1.26%	1.86%	1.34%	1.69%	1.34%
17mph	Phead	0.12%	0.00%	0.01%	0.00%	0.02%	0.00%	0.05%	0.02%
	Pchest	1.12%	0.58%	0.45%	0.29%	1.17%	0.49%	0.98%	0.39%
	Pneck	7.60%	5.95%	6.10%	5.72%	5.98%	5.19%	5.98%	5.38%
	Pfemur	0.48%	0.44%	0.46%	0.42%	0.47%	0.47%	0.47%	0.59%
	Pjoint	1.71%	1.02%	0.91%	0.71%	1.65%	0.95%	1.50%	0.99%

Note: Pneck was not used to calculate the Pjoint, because it dominated the Pjoint and over-predicted the injury risks.

As another example, the human-model-predicted Phead (based on HIC) and Pchest (based on chest deflection) subjected to the 35mph crash pulse with 4

pre-crash postures are shown in Figure 16. In the four parametric studies shown in Figure 16, the baseline designs were generally at a distance for the optimal

design. Table 8 shows the injury risks from the baseline design and the optimal designs predicted by the human model for all 12 delta-V*posture conditions.
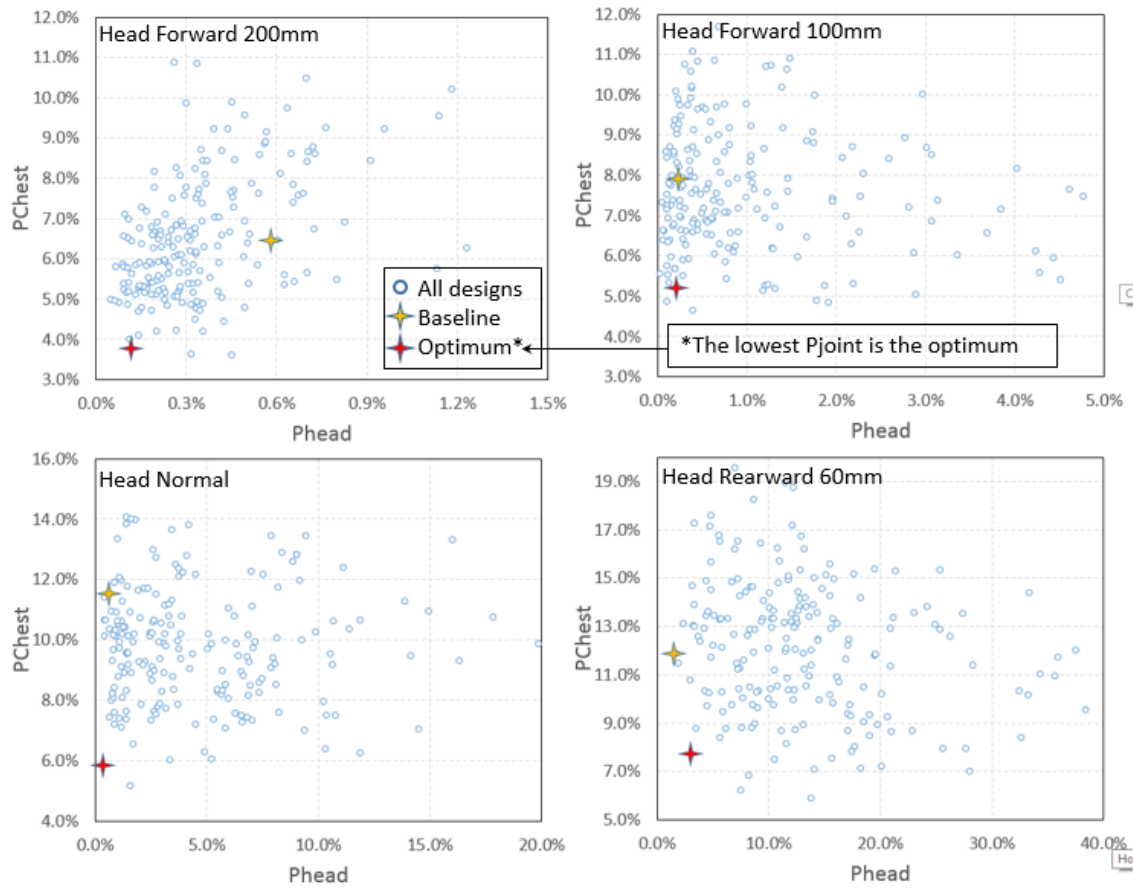

Figure 16: Human-model-predicted Phead and Pchest for 200 designs under the 35 mph crash pulse

Table 8: Human model-predicted injury risks for the baseline and optimal designs

		Head Forward (−200mm)		Head Forward (−100mm)		Normal (0 mm)		Head Rearward (+60mm)	
		Baseline	Optimal	Baseline	Optimal	Baseline	Optimal	Baseline	Optimal
35mph	Phead	0.58%	0.32%	0.25%	0.11%	0.42%	0.34%	1.68%	3.05%
	Pchest	6.43%	3.64%	7.84%	4.87%	11.42%	5.86%	11.90%	7.71%
	Pneck	6.96%	7.42%	6.71%	6.91%	8.20%	5.87%	8.38%	5.98%
	Pfemur	2.41%	1.10%	2.12%	0.95%	1.08%	1.37%	2.13%	1.40%
	Pjoint	9.22%	5.01%	10.01%	5.87%	12.74%	7.46%	15.23%	11.78%
25mph	Phead	0.84%	0.08%	0.12%	0.08%	0.05%	0.00%	0.04%	0.87%
	Pchest	3.95%	1.71%	4.29%	1.32%	5.57%	2.64%	4.82%	1.63%
	Pneck	7.07%	6.55%	6.53%	7.37%	7.72%	5.44%	7.68%	7.74%
	Pfemur	1.76%	0.86%	4.11%	1.19%	1.80%	1.30%	1.96%	1.18%
	Pjoint	6.43%	2.62%	8.33%	2.57%	7.31%	3.91%	6.73%	3.63%
17mph	Phead	0.11%	0.00%	0.06%	0.00%	0.01%	0.00%	0.00%	0.00%
	Pchest	2.85%	0.84%	2.35%	0.88%	2.31%	0.91%	2.66%	0.70%
	Pneck	7.64%	6.13%	7.24%	5.71%	6.40%	5.37%	5.86%	6.22%
	Pfemur	1.29%	0.82%	2.70%	0.92%	2.00%	0.88%	1.64%	0.94%
	Pjoint	4.21%	1.66%	5.04%	1.79%	4.27%	1.79%	4.25%	1.64%

Note: Pneck was not used to calculate the Pjoint, because it dominated the Pjoint and over-predicted the injury risks.

Figure 17 shows the injury risk reduction ratios at 12 delta-V*posture conditions, which are calculated by the (Pjoint_baseline–Pjoint_optimal)/Pjoint_baseline. The ATD model estimated the injury risk reduction to be the lowest at the 35mph with normal driving posture, and in general, further beyond that condition would result in higher injury risk reductions. The same trend cannot be found from the results using the human model. Interestingly, both the ATD model and the human model showed that postures with more forward head locations tend to have higher injury risk reductions than those with head being more rearward.
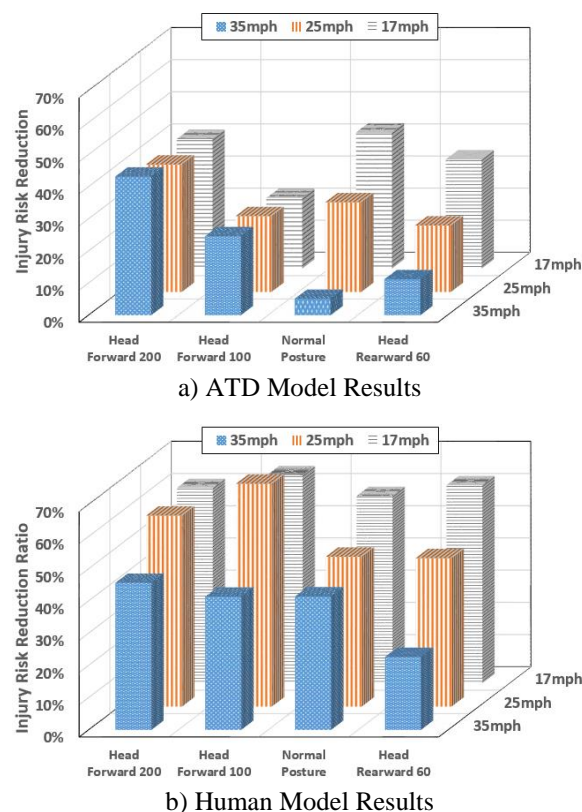

a) ATD Model Results

b) Human Model Results

Figure 17: Injury risk reduction ratios at different delta-V*posture conditions

INJURY RISK REDUCTION ESTIMATES

The field benefit evaluation combined results from the field data analysis, naturalistic driving data analysis, and the computational simulations. The occupant posture distribution change and the delta-V distribution change due to a DA or active safety system have been estimated by the naturalistic driving data analysis and the field data analysis in the previous sections, and the potential injury risk reductions at different combinations of delta-V and occupant pre-

crash posture have also been estimated by an ATD model and a human model. Therefore, the overall weighted injury risk reduction estimation of the integrated active and passive safety system can be estimated by the Eq 4:

$$Injury\_risk\_reduction\_ratio =$$
$$\sum_{i=1}^{Posture\_levels} \sum_{j=1}^{DeltaV\_levels} W_{ij} \times \left| \frac{P_{ij_{baseline}} - P_{ij_{optimal}}}{P_{ij_{baseline}}} \right| (4)$$

where W_{ij} is the weighting matrix developed in the field data analysis and the naturalistic driving data analysis. $P_{ij\_optimal}$ is the lowest probability of injury with the optimal passive safety design for an occupant in the given crash condition, while $P_{ij\_baseline}$ is the probability of injury with the baseline design for the occupant in the same crash condition. With different assumptions for the effectiveness of a DA or active safety system in reducing delta-V, different W_{ij} can be provided. In this equation, the summation can be changed to integration, if enough data points are collected.

To calculate the total injury risk reduction ratio, the injury risk reductions at different delta-Vs based on the delta-V distribution in Figure 5 were first weighted. Because the current MADYMO models cannot provide age effects, the three age groups in Figure 5 were combined. The weighted injury risk reduction ratios at different delta-Vs were combined in each head location. Finally, a weighted average of the injury risk reduction ratio was computed for the integrated active and passive safety system across the four head positions was computed.

The weights for head position were taken from the naturalistic driving data analysis (Figure 8). However, in that analysis, the amounts of forward and rearward excursion were not measured. The rearward excursion made up 11.67% of total time after braking and its effect was represented by the +60 head-excursion results. No head excursion was found 67.08% of the time, and forward head excursion occurred 21.25% of the time. This proportion was somewhat arbitrarily assigned 1/3 (or 7.08%) to the -200mm conditions and 2/3 (or 14.17%) to the -100mm condition. The results do change with head location, but this allocation is not expected to have a substantial effect on the final result.

Table 9 contains the risk reduction ratio for each head location and the overall risk reduction ratio based on the weighted average of the four head-excursion levels (as described above). The overall risk reduction is at 17% based on the ATD model and 48% based on the human model.

Table 9: Estimated percent reduction of total injury risks

Head location	Percent	Injury Risk Reduction	
		ATD Model	Human Model
Head forward (200mm)	7.08%	43%	58%
Head forward (100mm)	14.17%	25%	53%
Head neutral	67.08%	14%	47%
Head rearward (60mm)	11.67%	13%	44%
Overall weighted average		**17%**	**48%**

DISCUSSION

The application of a DA or active safety system may affect the delta-V and occupant pre-crash posture in motor vehicle crashes. In this study, a method combining field data analysis, naturalistic driving data analysis, and computational simulations was developed to investigate the effect of a DA or active-safety-system-induced delta-V and occupant pre-crash posture changes on occupant injury risks in frontal crashes.

In the field data analysis, the basic assumption in this study is that the DA or active safety system can avoid 20% of the frontal crashes. In the literature, the forward collision warning system is the most frequently studied pre-collision system. A review of intelligent transport systems by Bayly et al. (2007) estimated the percentage of frontal crashes that can be prevented by such a system varied significantly (ranging from 7% to 80%) from study to study. Two recent studies by Kusano and Gabler (2010, 2012) provided more conservative estimates, predicting that only 0-14% of the frontal crashes can be prevented by the pre-collision systems. Based on the literature, we believe that the assumption of 20% of the frontal crashes being prevented by the DA or active safety system is reasonable. However, different percentage values can be used by the same method developed in this study, which will likely affect the final injury risk reduction estimation.

In this study, naturalistic driving data were used to quantify the occupant head location change during a hard braking event, and the resulted head location patterns were used to estimate the potential advantage of an integrated active and passive safety system. Therefore, this study only focused on a forward collision warning system, not on an autonomous braking system. While a forward collision warning system is designed to warn the driver before a potential crash, autonomous braking system is designed to brake, even if there is no driver input. If the driver is not aware of the brake, he/she will likely move forward in the braking event due to the body inertia. As a result, the head location changes will be very different to those estimated in the current study.

In this study, difference of injury risk reduction estimates existed between the ATD model (predicted 17% injury reduction) and the human model (predicted 48% injury reduction), but they have also shown some consistent trends. In particular, both models predicted that the injury reduction is higher when the head is closer to the steering wheel. This is likely due to two reasons: 1) The normal driving posture is generally optimized and the head location in the "head rearward" condition is only 60 mm rearward from the normal driving location, therefore the room for reducing the injury risk is limited in those conditions; 2) the current restraint design space is constrained by regulatory and public domain crash test protocols that mainly focus on normal driving posture, thus design parameters, such as the airbag tether length in the baseline design is very close to the maximum. A larger range of design parameters with adaptive features specifically for more rearward occupants may further improve the injury risk reduction potential.

Using the ATD model, in a 35 mph crash, the baseline restraint design is very close to the optimal protection to an occupant in a normal driving posture, because it is the NCAP crash condition. However, the same restraint system is not optimal when the human model is used. Given the fact that the main target of the baseline restraint design is to reduce the injury risks from the ATD, it is reasonable that higher injury risk reduction was estimated by the human model than the ATD model.

There are several limitations in this study. First, we only used a single vehicle and pure frontal barrier crash conditions. A wider range of vehicle models and crash conditions may cover the field conditions better. Second, in our naturalistic driving data analysis, the head positions were only categorized into groups, but the exact positions were not quantified. Further research is necessary to accurately quantify the head positions before and after breaking events. Third, both the ATD model and human model have certain limitations in terms of injury risk prediction. Compared to the field data, the ATD model under-estimated the chest and KTH injury risks, while the human model has to adjust the chest injury risk curves

to match the field data. Moreover, active muscle forces were not yet considered in the current study, and future studies using human models with active muscle forces (Meijer et al. 2013; Osth et al. 2015) might be necessary to better predict the injury risks, especially for lower extremities. Lastly, occupant stature, weight, gender, and age variations were not considered in this study. Because of the limitations of the MADYMO human model, such effects are very difficult to be considered in the current study. Future study using parametric human finite element models (Hu et al. 2012; Schoell et al. 2015; Shi et al. 2015; Wang et al. 2015) may be necessary to further investigate the potential field capability of the integrated active and passive safety system. Nonetheless, this study demonstrated promising potential of an integrated active and passive safety system for reducing injury risks in frontal crashes.

CONCLUSIONS

In this study, a method was developed using the field data to estimate the delta-V distribution change by assuming a 20% crash avoidance by DA or active safety systems. The patterns of driver head location changes in hard braking events were estimated based on a naturalistic driving data analysis. It was found that drivers' head position were mostly in the center position before the braking onset, while the percentage of time drivers leaning forward or backward were increased significantly after the braking onset. Significant age effect was also observed. Simulations were performed with MADYMO HIII ATD model as well as the MADYMO human model to investigate potential injury risk reduction if the restraint system is optimized to adapt to different delta-Vs and occupant pre-crash postures. By combining the results for the delta-V and head position distribution changes, a weighted average of injury risk reduction of 17% and 48% was predicted by the 50th percentile ATD model and human body model, respectively, assuming the restraint system can adapt to the specific delta-V and pre-crash posture. This study demonstrated the potential capability of integrated active and passive safety systems for injury risk reduction in frontal crashes.

ACKNOWLEDGMENTS

REFERENCES

Adam, T. and Untaroiu, C.D. (2011) Identification of occupant posture using a Bayesian classification methodology to reduce the risk of injury in a collision. *Transport Res C-Emer* 19(6): 1078-1094.

Augenstein, J., Perdeck, E., Stratton, J., Digges, K. and Bahouth, G. (2003) Characteristics of crashes that increase the risk of serious injuries. *Annu Proc Assoc Adv Automot Med* 47: 561-576.

Bayly, M., Fildes, B., Regan, M. and Young, K. (2007) Review of crash effectiveness of intelligent transport systems. Project No 027763 - TRACE Deliverable D4.1.1-D6.2.

Bean, J.D., Kahane, C.J., Mynatt, M., Rudd, R.W., Rush, C.J. and Wiacek, C. (2009) Fatalities in frontal crashes despite seat belts and air bags – review of all CDS cases – model and calendar years 2000-2007 – 122 fatalities. National Highway Traffic Safety Administration, DOT HS 811 202.

Bose, D., Crandall, J.R., Untaroiu, C.D. and Maslen, E.H. (2010) Influence of pre-collision occupant parameters on injury outcome in a frontal collision. *Accid Anal Prev* 42(4): 1398-1407.

Digges, K., Dalmotas, D. and Prasad, P. (2013) An NCAP star rating system for older occupants. In The 23rd International Technical Conference on the Enhanced Safety of Vehicles (ESV), Seoul, Republic of Korea.

Evans, L. (1986) The effectiveness of safety belts in preventing fatalities. *Accid Anal Prev* 18(3): 229-241.

Evans, L. (1991) Airbag effectiveness in preventing fatalities predicted according to type of crash, driver age, and blood alcohol concentration. *Accid Anal Prev* 23(6): 531-541.

Farmer, C.M. (2005) Relationships of frontal offset crash test results to real-world driver fatality rates. *Traffic Inj Prev* 6(1): 31-37.

Flannagan, C. (2013) A method for estimating delta-V distributions from injury outcomes in crashes. UMTRI Report No 2013-15.

Hu, J., Rupp, J. and Reed, M. (2012) Focusing on vulnerable populations in crashes: recent advances in finite element human models for injury biomechanics research. *Journal of Automotive Safety and Energy* 3(4): 295-307.

Hu, J., Wu, J., Klinich, K.D., Reed, M.P., Rupp, J.D. and Cao, L. (2013a) Optimizing the rear seat

environment for older children, adults, and infants. *Traffic Inj Prev* 14 Suppl: S13-22.

Hu, J., Wu, J., Reed, M.P., Klinich, K.D. and Cao, L. (2013b) Rear seat restraint system optimization for older children in frontal crashes. *Traffic Inj Prev* 14(6): 614-622.

Ito, D., Ejima, S., Sukegawa, Y., Antona, J., Ito, H. and Komeno, F. (2013) Assessment of a pre-crash seatbelt technology in frontal impacts by using a new crash test sled system with controllable pre-impact braking. In The 23rd International Technical Conference on the Enhanced Safety of Vehicles (ESV), Seoul, Republic of Korea.

Kahane, C. (1996) Fatality reduction by air bags: Analysis of accident data through early 1996. NHTSA, U.S. Department of Transportation, Report HS 808 470, Washington, DC.

Kahane, C. (2000) Fatality reduction by safety belts for front-seat occupants of cars and light trucks. NHTSA, U.S. Department of Transportation, Report HS 809 199, Washington, DC.

Komeno, F., Koide, T., Miyagawa, T., Saito, T., Sukegawa, Y., Ito, D., Asaoka, M. and Yamada, H. (2013) Crash sled test based evaluation of a pre-crash seatbelt and an airbag to enhance protection of small drivers in vehicles equipped with autonomous emergency braking systems. In The 23rd International Technical Conference on the Enhanced Safety of Vehicles (ESV), Seoul, Republic of Korea.

Kononen, D.W., Flannagan, C.A. and Wang, S.C. (2011) Identification and validation of a logistic regression model for predicting serious injuries associated with motor vehicle crashes. *Accident Analysis and Prevention* 43(1): 112-122.

Kramer, A.F., Cassavaugh, N., Horrey, W.J., Becic, E. and Mayhugh, J.L. (2007) Influence of age and proximity warning devices on collision avoidance in simulated driving. *Hum Factors* 49(5): 935-949.

Kusano, K.D. and Gabler, H.C. (2010) Potential occupant injury reduction in pre-crash system equipped vehicles in the striking vehicle of rear-end crashes. *Ann Adv Automot Med* 54: 203-214.

Kusano, K.D. and Gabler, H.C. (2012) Safety benefits of rorward collision warning, brake assist, and autonomous braking systems in rear-end collisions. *IEEE T Intell Transp* 13(4): 1546-1555.

Lerner, N.D. (1993) Brake perception-reaction times of older and younger drivers. Proceedings of the

Human factors and Ergonomics society 37th Annual Meeting, pp. 206-210.

Mages, M., Seyffert, M. and Class, U. (2011) Analysis of the pre-crash benefit of reversible belt pre-pretensioning in different accident scenarios. In The 22nd International Technical Conference on the Enhanced Safety of Vehicles (ESV), Washington, D.C.

Meijer, R., Elrofai, H., Broos, J. and Hassel, E.V. (2013) Evaluation of an active multi-body human model for braking and frontal crash events. In The 23rd International Technical Conference on the Enhanced Safety of Vehicles (ESV), Seoul, Republic of Korea.

Merz, U., Schöneburg, R., Fehring, M., Bachmann, R. and Heinrich, T. (2013) PRE-SAFE® impulse – early interacting occupant restraint system. In The 23rd International Technical Conference on the Enhanced Safety of Vehicles (ESV), Seoul, Republic of Korea.

NHTSA (1999) Fourth report to Congress—effectiveness of occupant protection systems and their use. . National Highway Traffic Safety Administration, U.S. Department of Transportation, Washington, DC.

NHTSA (2001) Fifth/Sixth report to Congress—effectiveness of occupant protection systems and their use. . National Highway Traffic Safety Administration, U.S. Department of Transportation, Washington, DC.

Osth, J., Brolin, K. and Brase, D. (2015) A human body model with active muscles for simulation of pretensioned restraints in autonomous braking interventions. *Traffic Injury Prevention* 16: 304-313.

Ryb, G.E., Burch, C., Kerns, T., Dischinger, P.C. and Ho, S. (2010) Crash test ratings and real-world frontal crash outcomes: a CIREN study. *J Trauma* 68(5): 1099-1105.

Sayer, J., LeBlanc, D., Bogard, S., Funkhouser, D., Bao, S., Buonarosa, M.L. and Blankespoor, A. (2011) Integrated vehicle-based safety systems field operational test final program report. University of Michigan Transportation Research Institute, Ann Arbor, MI.

Schoell, S.L., Weaver, A.A., Vavalle, N.A. and Stitzel, J.D. (2015) Age- and sex-specific thorax finite element model development and simulation. *Traffic Inj Prev* 16 Suppl 1: S57-65.

Segui-Gomez, M., Lopez-Valdes, F.J. and Frampton, R. (2007) An evaluation of the EuroNCAP crash test safety ratings in the real world. *Annu Proc Assoc Adv Automot Med* 51: 282-298.

Segui-Gomez, M., Lopez-Valdes, F.J. and Frampton, R. (2010) Real-world performance of vehicle crash test: the case of EuroNCAP. *Inj Prev* 16(2): 101-106.

Shi, X., Cao, L., Reed, M.P., Rupp, J.D. and Hu, J. (2015) Effects of obesity on occupant responses in frontal crashes: a simulation analysis using human body models. *Computer Methods in Biomechanics and Biomedical Engineering* 18(12): 1280-1292.

Stigson, H., Kullgren, A. and Rosen, E. (2012) Injury risk functions in frontal impacts using data from crash pulse recorders. *Ann Adv Automot Med* 56: 267-276.

TASS (2012) MADYMO Human Body Models Manual Release 7.4.2. *TNO*.

Untaroiu, C.D. and Adam, T.J. (2012) Occupant classification for an adaptive restraint system: the methodology and benefits in terms of injury reduction. IRCOBI Conference Proceedings - International Research Council on the Biomechanics of Injury.

Wang, Y., Bai, Z., Cao, L., Reed, M.P., Fischer, K., Adler, A. and Hu, J. (2015) A simulation study on the efficacy of advanced belt restraints to mitigate the effects of obesity for rear-seat occupant protection in frontal crashes. *Traffic Inj Prev* 16 Suppl 1: S75-83.

APPENDIX A: A METHOD FOR ESTIMATING DELTA-V DISTRIBUTIONS FROM INJURY OUTCOMES IN CRASHES

The proposed approach to estimate delta-V depends on two assumptions. First, the delta-V distribution can be modeled with a parametric form that will hold for different classes of crashes, though each class of crashes will have different parameters. Second, the relationship between delta-V and injury is fixed for a given impact direction, and that relationship will hold for the general population of vehicles involved in impacts in the same direction.

The estimation process itself requires three elements:
1) Injury risk curve for a specific damage location
2) Distributional form for delta-V
3) Injury distribution for occupants in target crashes

The injury risk curve captures the relationship between delta-V and injury. Delta-V describes the severity of the crash as experienced by a given vehicle, and injury risk is related to crashworthiness. Since crashworthiness differs for different parts of the vehicle structure, this relationship must be modeled for a specific crash direction. Since CDS contains delta-V estimates as well as multiple measures of injury severity (AIS and KABCO), it can be used to develop injury risk curves.

Choosing an appropriate statistical distribution reduces the number of parameters needed to define the model. In general, a lognormal distribution describes the CDS delta-V distributions well. There should be fewer parameters in the delta-V distribution than there are levels of injury. The lognormal has two free parameters.

The distribution of injury levels is the data-based target of the fitting process. The injury distribution is the percentage of occupants who sustain injury at each level. Since there are several available injury scales (e.g., AIS, KABCO), it is important to use the same injury outcome measure for both the injury risk curves and the empirical injury distribution. When using GES or FARS, the injury coding system will be the KABCO scale. Even though AIS is a more precise injury scoring system, the injury risk curves from CDS should predict risk on the KABCO scale. If AIS scoring is available in the injury data source (e.g., a hospital database that has injury outcome but few or no crash details), CDS-based risk curves should predict risk of AIS injury levels instead. In this paper, only KABCO-based estimation is demonstrated.

Estimation

The first step in estimation is to sort crashes by damage areas in a manner that can be achieved in both CDS and GES. The second step is to generate the risk curves for the each crash type. In this paper, the risk curves are based on cumulative logistic regression using log-transformed delta-V as the predictor and KABCO injury level as the outcome variable. Cumulative logistic regression is an extension of binary logistic regression, which fits one or more predictors to a binary outcome. The logistic regression model is given by Equation A1.

$$p = {1}/{1 + \exp(-(\beta_0 + \sum_i \beta_i x_i))} \quad \text{(A1)}$$

where, p is the estimated probability of the outcome (e.g., injury),

β_0 is the intercept, and

β_i are the estimated coefficients of each predictor, x_i, $i=1..r$ where r is the number of predictors in the equation

Cumulative logistic regression is essentially the same as logistic regression except that it allows more than two ordered categories of outcome. The model creates a series of increasing cutpoints among the ordered categories and fits a single slope parameter for each x_i and a separate intercept for each cutpoint. Thus when KABCO is the outcome variable and ln delta-V is the predictor, the model fits a single slope parameter for ln delta-V and separate intercepts for four cutpoints: K (vs. ABCO), KA (vs. BCO), KAB (vs. CO), and KABC (vs. O). The advantage of the cumulative model (rather than other possible choices such as generalized logit) is that the predicted risk of more severe injury is always lower than the predicted risk of less severe injury, which generally describes real-world injury patterns.

The joint distribution of each injury level in the database is the product of the risk of injury at each delta-V and the probability of experiencing that delta-V in a crash. As an example, Figure A1 shows a lognormal delta-V distribution with parameters μ=2.0 and σ=0.4 that might represent the probability of experiencing a frontal crash at each delta-V.

Figure A2 shows the same delta-V distribution plotted with the KA injury risk curve and their joint distribution (the product at each delta-V value). Figure A3 shows the joint injury distribution for each injury level.
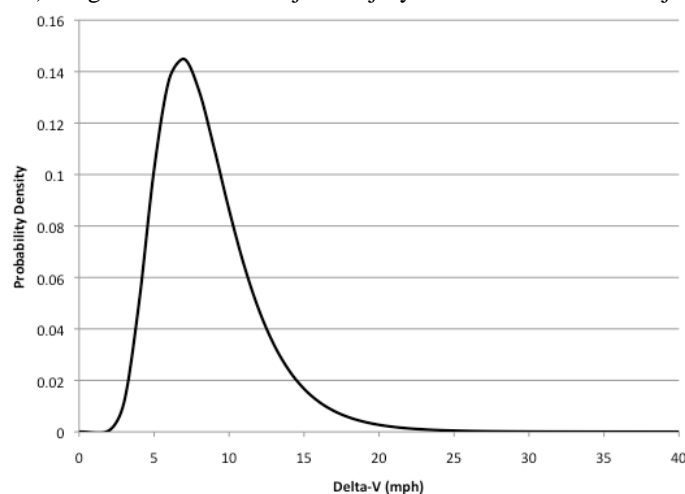

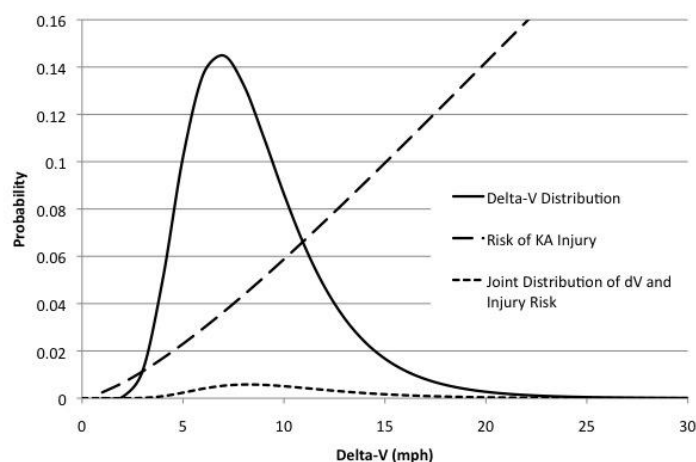Figure A1: Example of lognormal delta-V distribution. In this graph, μ=2.0 and σ=0.4.

Figure A2: Injury risk curve for KA injuries, distribution of crash severity, and the distribution of injury KA injury probability (the product of injury risk and crash severity distribution.)
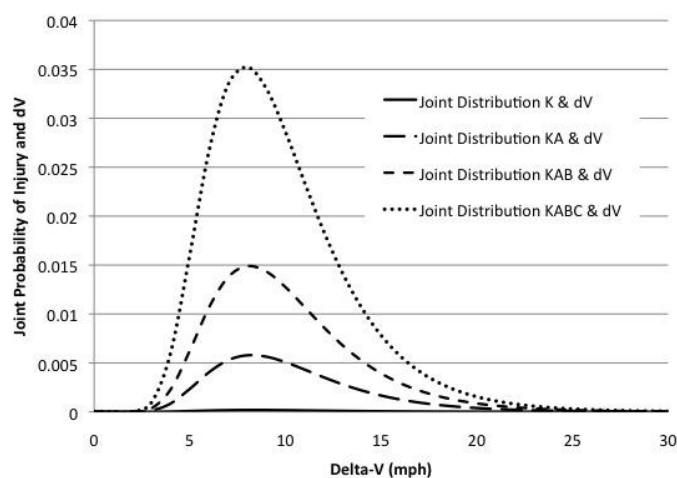

Figure A3: Joint risk of being in a crash with a given delta-V and injured (at each injury level).

For each of the joint distributions in Figure A3, the area under the curve represents the total risk of the group of injury levels (e.g., KAB). Since each outcome is cumulative, the area *between* the curves represents the total risk of a specific (non-cumulative) outcome (e.g., B injury only). The remaining probability (1 minus probability of any injury) is the probability of no injury. Thus the proportion of injuries among K, A, B, C, and O can be estimated using these products of the injury risk model and a given delta-V distribution.

If the injury-risk curves based on CDS models are considered fixed, then the only free parameters in the system illustrated in Figure A3 are those that describe the delta-V distribution. If the KABCO injury distribution is known for a dataset but the delta-V distribution is not, different values of μ and σ defining the delta-V distribution can be tested until the product of the injury risk and delta-V curves come as close as possible to the target (data-based) proportions of K, A, B, C, and O injuries.

Because the injury distribution has four degrees of freedom (the fifth injury level is constrained to sum to 1) and the delta-V distribution has two degrees of freedom, not all injury distributions can be perfectly recovered with this system. As a result, we need a loss function to score the match between the injury distributions in the target dataset and those predicted by the product of injury risk and delta-V distribution.

The chi-square test statistic is a common measure of correspondence between model and data for a contingency table and is suitable for this application. The equation for the chi-square statistic is given in Equation A2. The parameters that minimize this loss function are selected for the delta-V distribution that results from the estimation process.

$$X^2 = \sum_i \frac{(o_i - e_i)^2}{e_i} \qquad (A2)$$

where

   o is the observed cell proportion,
   e is the expected cell proportion (from lognormal model), and
   i sums over the five cells in the table (one for each injury level)

Validation

The performance of the method is tested in two ways. First, a simulation explores issues related to bias and required sample size for use of the method. Each run of the simulation involved generating a sample of simulated injury levels for 100, 1000, or 5000 cases and then using the delta-V estimation method described above to estimate the parameters of the underlying delta-V distribution.

Each case in the simulation was generated in two steps, each of which corresponds to the model assumptions underlying the method. First, a value of delta-V was selected at random from a lognormal distribution with parameters μ=3.0 and σ=0.7. Next, an injury level on the KABCO scale was selected at random based on the risk model developed from CDS and the delta-V value selected in the first step. Once a simulated sample was generated, the empirical distribution of injury levels for that sample was returned. Based only on the distribution of the five injury levels, along with the fixed injury risk curves, the method described above was used to estimate the parameters of the delta-V distribution for each simulated sample. The process was repeated 100 times for each sample size.

Second, to explore the performance of the method on real data, the model was used to estimate the parameters of the delta-V distribution for frontal cases in the CDS database (where delta-V distribution is known.) The outcome of the injury-based estimation process is compared to both a direct sample estimate of the parameters of the lognormal delta-V distribution from CDS and the purely empirical (non-parametric) distribution of delta-V from the same cases.

These validation efforts do not push the boundaries of the underlying assumptions of the model. The simulation uses the assumed model to produce test data and the CDS comparison is to the same data from which the injury risk curves are developed. However, there are infinitely many ways the model can be wrong relative to real-world data, so it is appropriate to limit the scope of this paper to testing the model under friendlier conditions. Future work should explore the robustness of the model to violations of its underlying assumptions.

Validation Results

Delta-V Distribution Form
The typical method of testing the fit of a distributional form to data is the Kolmogorov-Smirnoff test. However, this method does not work with a stratified, weighted sample. Instead, graphical methods were used to look at the relationship between the delta-V distribution for frontals (defined as general area of damage (GAD1) equal to "F") in CDS and a variety of candidate distributions.

The lognormal distribution fits the delta-V distribution for classes of crashes fairly well. Figure A4 shows how ln delta-V for frontals in CDS is related to the normal distribution. (Comparing the log of delta-V to the normal distribution is equivalent to comparing delta-V to the lognormal distribution.) Specifically, the proportion of the delta-V distribution for frontal crashes was computed for bins in 1 mph increments. This proportion was cumulated and compared to the z-score associated with the cumulative proportion of each delta-V bin. The straight line in Figure A4 between the normal variate and ln(delta-V) indicates that the lognormal distribution is a good fit to delta-V in frontals in CDS. Additional investigation of delta-V distributions indicated that the lognormal is a good fit for other crash modes as well. The gamma distribution was also a good candidate but was not used in this paper.
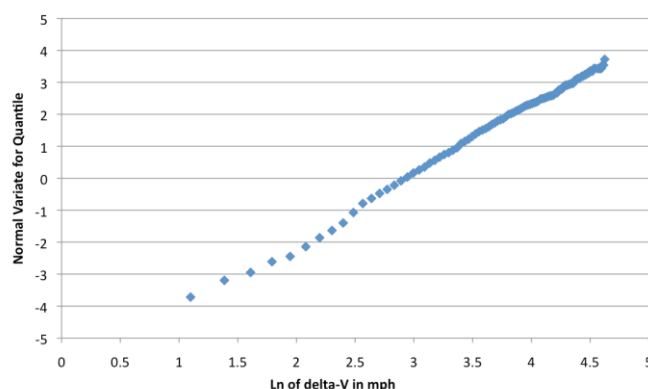

Figure A4: Plot of normal variates for each quantile vs. ln delta-V (in mph).

Injury Risk Curves
Injury risk curves using cumulative logistic regression to identify risk of KABCO injury outcome as a function of delta-V for vehicles with frontal damage in CDS are shown in Table A1 and Figure A5. There is a single coefficient for log-transformed delta-V and a separate intercept for each level of injury (cumulated). No other potential injury predictors were considered in the model, so they reflects the distribution of age, gender, and belt use found in CDS and GES. The risk curves have a common slope, and each successive intercept predicts the probability of a given level or worse injury. For example, the "B" intercept of -4.9928 determines the risk of K, A, or B injury as a function of delta-V in a frontal impact.

Table A1: Coefficients and Fit Statistics for Injury Model in Frontal Impacts

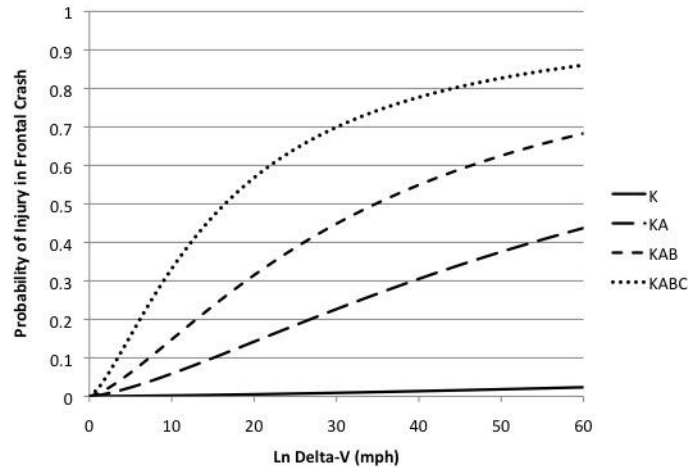| Analysis of Maximum Likelihood Estimates						
Parameter		**DF**	**Estimate**	**Standard Error**	**Wald Chi-Square**	**Pr > ChiSq**
Intercept	**K**	1	-9.4901	0.3145	910.4918	<.0001
Intercept	**A**	1	-6.0136	0.6559	84.0483	<.0001
Intercept	**B**	1	-4.9928	0.3382	217.9715	<.0001
Intercept	**C**	1	-3.9414	0.2559	237.2877	<.0001
Ln (delta-V mph)		1	1.4070	0.1056	177.6847	<.0001

Figure A5: Cumulative logistic risk models for KABCO injuries in frontal impacts. Each line represents the risk of the group of injury levels for a given delta-V value.

Simulation

The arbitrary parameters of the simulation were μ=3.0 and σ=0.7, and three sample-size scenarios were tested for the injury data: 100, 1000, and 5000 cases. Figure A6 shows the distribution of the estimated mean of the delta-V distribution for simulated samples sizes of 100, 1000, and 5000 crashes. The estimation process becomes more precise as sample size goes up. In addition, there is no evidence of bias as the average estimate for all three sample sizes was 3.0.
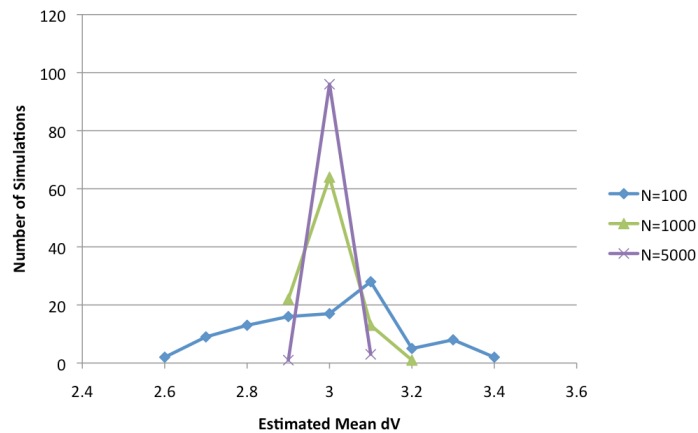

Figure A6: Simulation results for estimation of mean delta-V. The true value is 2.0.

Figure A7 shows the distribution of estimated standard deviation of the delta-V distribution for simulated samples sizes of 100, 1000, and 5000 crashes. As with estimating the mean value, the estimation process becomes more precise as sample size goes up. However, standard deviation is more difficult to estimate precisely and the results are more varied. At a sample size of 100, the estimation method frequently reaches the end of the search space, suggesting that the estimates are not stable for such a small sample size. The standard deviation estimates for sample sizes of 100, 1000, and 5000 were 0.65, 0.69, and 0.70, respectively. This suggests that the approach is unbiased for standard deviation as well, but sufficient sample size is required to have a stable estimate.
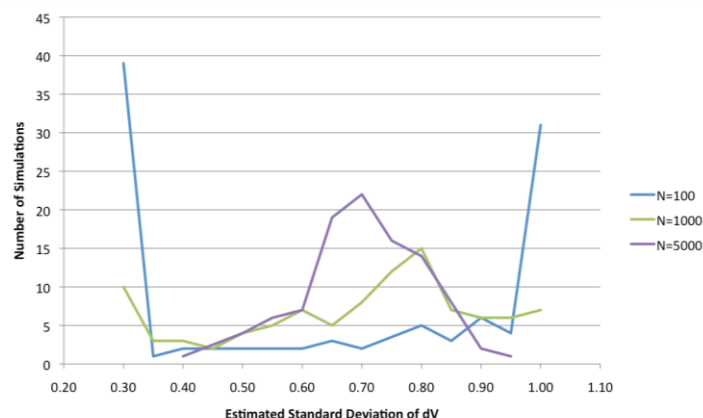
Figure A7: Simulation results for estimation of standard deviation of delta-V. The true value is 0.7.

Estimation of CDS Delta-V Distribution

When the estimation approach was applied to the injury distribution from CDS frontals, the resulting parameters to define the delta-V distribution were $\mu=2.47$ and $\sigma=0.43$. The parameters developed from the actual data were $\mu=2.43$ and $\sigma=0.44$. Table A2 shows the empirical (weighted) distribution of injury for CDS frontals (with non-missing delta-V). The last column shows the estimated injury distribution, based on the best-fit lognormal parameters and the embedded risk models for frontal crashes. The proportions match quite well with X^2=xxx.

Table A2: Empirical and Estimated Proportion of KABCO Injuries for Frontals in CDS

Injury Level	Empirical Proportion of Cases	Estimated Proportion of Cases ($\mu=2.47$, $\sigma=0.43$)
K	60.59%	60.62%
A	19.82%	19.88%
B	11.20%	11.08%
C	8.10%	8.12%
O	0.29%	0.30%

Figure A8 shows three distributions for comparison. The solid black line is the weighted cumulative distribution of delta-V from frontal cases in CDS. The dashed gray line shows the lognormal distribution calculated directly from the data in CDS. The dotted gray line shows the lognormal distribution estimated using the injury-risk-curve approach. The correspondence of all three distributions is quite close, suggesting that the injury-based approach proposed in this paper works well.
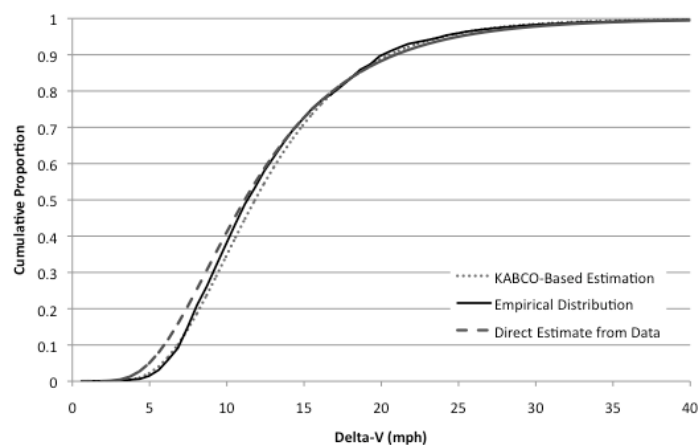

Figure A8: Three distributions of delta-V for frontal crashes in CDS. Solid line represents empirical delta-V cumulative curve. Dashed line is the lognormal distribution estimated directly from the data, and the dotted line is the lognormal distribution estimated only from the injury distribution.

APPENDIX B: DETAILS OF COMPUTATION FOR RANDOM-SHIFT MODEL

Let X and Y be independent, continuous, and positive random variables. Then

$$
\begin{aligned}
P(X - Y \leq 0) &= \iint\limits_{x-y \leq 0} f(x,y) \, dy \, dx \\
&= \int_0^\infty \int_x^\infty f(x) \, f(y) \, dy \, dx \\
&= \int_0^\infty f(x) \left[\int_x^\infty f(y) \, dy \right] dx \\
&= \int_0^\infty f(x) \left[1 - F_Y(x) \right] dx
\end{aligned}
$$

Suppose X is lognormal with parameters μ and σ^2 and Y is exponential with rate λ. Then

$$
1 - F_Y(x) = e^{-\lambda x}
$$

and

$$
P(X - Y \leq 0) = \int_0^\infty e^{-\lambda x} f_X(x) \, dx = E_X\!\left[e^{-\lambda X} \right]
$$

If we set this probability equal to 0.43, we can find the root of

$$
g(\lambda) = \int_0^\infty e^{-\lambda x} f(x) \, dx - 0.43 = 0
$$

as a function of λ. The R code is shown below for $\mu = 2.0$ and $\sigma = 0.4$.

```
fun1 <- function(lam) {
  fun2 <- function(x) {
    exp(-lam*x) * dlnorm(x,mean=2.0,sd=0.4) }
  integrate(fun2,lower=0,upper=Inf)$value - 0.43 }

uniroot(fun1,c(0,1))
```

The result is $\lambda = 0.1131$. The plot below shows the function $g(\lambda)$ and the root at 0.1131.

Note that the moment generating function of a random variable X is
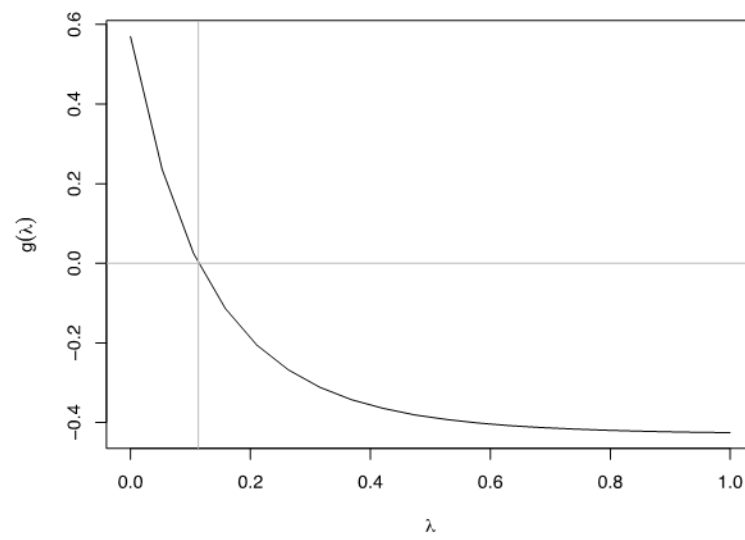
$$
M_X(t) = E\!\left[e^{tX} \right]
$$

and that

$$
P(X - Y \leq 0) = E\!\left[e^{-\lambda X} \right] = M_X(-\lambda)
$$

Instead of a lognormal, if we are willing to allow X to have a gamma distribution with parameters α and β, the moment generating function is

$$
M_X(t) = \left(\frac{\beta}{\beta - t} \right)^\alpha \qquad\qquad t < \beta
$$

and

$$
M_X(-\lambda) = \left(\frac{\beta}{\beta + \lambda} \right)^\alpha \qquad\qquad -\lambda < \beta
$$

Setting the above equation equal to 0.43 and solving for λ gives

$$\lambda = \frac{\beta \left[1 - (0.43)^{1/\alpha} \right]}{(0.43)^{1/\alpha}}$$

APPENDIX C: CHEST DELFECTION COMPARISON BETWEEN MADYMO AND THUMS HUMAN MODELS

Because it is almost impossible to use whole-body cadaver tests with the restraint systems used in this study to validate the MADYMO human model, in this study a finite element human model (THUMS 4.0) was used to cross-validate the chest deflection results from the MADYMO human model. Because the finite element model was not available for the same vehicle as used in the MADYMO model, a rear-seat model that was developed and validated in a previous study in both MADYMO and Ls-dyna was used.

Figure C1 shows the MADYMO and Ls-dyna human models in a rear-seat compartment. The rear-seat and seat belt models in both formats have been validated against a 35 mph sled test using a HIII 50th ATD. In the validation sled test, the floor pan of the vehicle under the rear seat was removed and replaced with a simple sheet metal box section, reinforced with foam board inside. Therefore, the seat in the MADYMO and Ls-dyna models were tuned to match the test results. The rear-seat model was integrated with a validated TRW three-point seatbelt model, which includes a load limiter, retractor pre-tensioner, and anchor pre-tensioner.
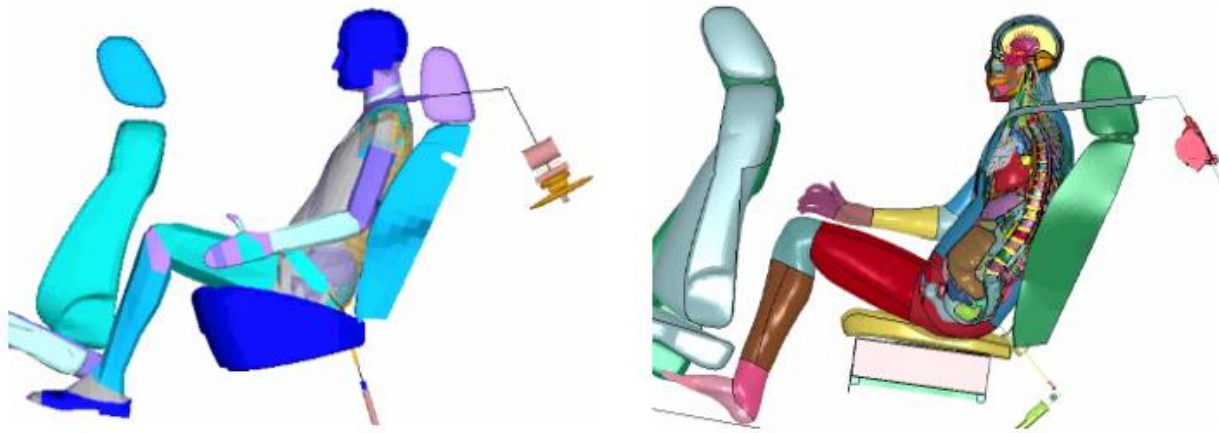

Figure C1: MADYMO (left) and Ls-dyna (right) human models in a rear-seat compartment

In this study, three MADYMO simulations and three Ls-dyna simulations under the restraint conditions described in Table C1. The chest deflections in each simulation were measured at four locations on the chest, and the results are shown in Table C1 as well. The ratios between the MADYMO-model-predicted chest deflection and THUMS-predicted chest deflection were from 1.18 to 4.98, while the ratios for the maximal chest deflections were from 1.18 to 1.44. In this study a ratio of 1.50 was decided to be used to scale down the chest deflections predicted by the MADYMO human model. This adjustment has resulted in much better match between the simulated chest injury risks and those in the field as shown in Table C2.

Table C1: Chest deflection comparison between MADYMO human model and THUMS

Restraint Condition	ChestD (mm)	MADYMO model	THUMS	Ratio MADYMO/THUMS
6kN load limit Retractor pretensioner Buckle pretensioner	ChestD1	50.3	35.5	1.42
	ChestD2	43.3	17.8	2.43
	ChestD3	39.3	17.7	2.22
	ChestD4	29.3	7.6	3.86
4kN load limit Retractor pretensioner	ChestD1	50.6	35.1	1.44
	ChestD2	41.7	20.5	2.03
	ChestD3	31.7	9.8	3.23
	ChestD4	28.4	5.7	4.98
2.5kN load limit Retractor pretensioner Buckle pretensioner	ChestD1	37.1	31.4	1.18
	ChestD2	30.1	18.8	1.60
	ChestD3	29.0	16.8	1.73
	ChestD4	26.5	10.0	2.65

Table C2: Human-model predicted chest injury risks at different crash speeds

Velocity	ChestD (mm)	Pchest	ChestD-Scaled (mm)	Pchest-Scaled	AIS3+ Chest Injury Risks using NASS-CDS data
17mph	36.1	8.4%	24.1	2.3%	1.2%-2.6%
25mph	47.5	16.8%	31.7	5.6%	5.0%-10.2%
35mph	58.5	39.5%	39.0	11.4%	8.7%-17.1%

The NASS-CDS result was based on a recent UMTRI field analysis, which is not published yet.